# The study of visible and near-infrared absorber based on Multi- layer metamaterial structure

**Zichun Li, Jinhua Li*, Ye Zhang, Yingjiao Zhai, Xueying Chu, Yu Zhang**

International Joint Research Center for Nanophotonics and Biophotonics, Nanophotonics and Biophotonics Key Laboratory of Jilin Province, School of Science, Changchun University of Science and Technology, Changchun, 130022, P.R. China

* Corresponding author: lijh@cust.edu.cn

**Keywords:** broadband absorber, multi-layer metamaterials, near-infrared

**Abstract:** We propose a design of a broadband absorber based on a multi-layer metamaterial nanostructure composed of a periodic array of silver-silica-silver (Ag-SiO2-Ag) cubes and a silver (Ag) bottom film. The proposed structure can achieve nearly perfect absorption with an average absorbance of 97% spanning a broad range from visible to near-infrared (i.e.,from 600 nm to 1300 nm), showing a 90% absorption bandwidth over 412 nm, and the peak absorption is up to 99.8%. The excitation of superior surface plasmon resonance combined with the resonance induced by the metal-insulator-metal Fabry-Perot (FP) cavity leads to this broadband perfect absorption. The polarization and angle insensitivity is demonstrated by analyzing the absorption performance with oblique incidences for both TE- and TM-polarized waves. In addition, we discuss the impact of various metal materials and geometry structure on absorption performance in detail. The proposed broadband metamaterial absorber shows a promising prospect in applications such as solar cell, infrared detection, and imaging. Moreover, the use of a thin titanium cap and an aluminum film instead of noble metals has the potential to reduce production cost in applications.

## 1. Introduction

Metamaterial devices have attracted substantial attention due to their marvelous electromagnetic performance in many applications such as antenna systems [1], [2], electromagnetic cloaking [3,], imaging [4], ultra-sensitive sensing [5] and refractive index engineering [6]. The subwavelength structure of the metamaterials[7] can be tailored flexibly by designing the artificial “meta-atoms”.[8] This characteristic enables the metamaterials[9] a designable permittivity[10] and permeability[11]. Meanwhile, the performance of the energy [12] depletion in metamaterials can be utilized in a positive way to design metamaterial[13] absorbers by introducing the power loss[14].

During the last decade, trends to achieve light absorption in metamaterials[15] and plasmonic[16] nanostructures have increased tremendously due to the huge interest in the development[17] of solar energy harvesting[18]. Generally, regarding the absorption bandwidth, absorbers can be categorized into two types [19], namely narrow band absorber and broadband absorber [20]. The former one can easily find applications in linear or nonlinear sensors covering both visible and infrared regions [21]. On the contrary, in the applications such as photodetectors [22], thermal emitters [23], photovoltaics (PV) [24] and ultra-short pulse generation [25], broadband absorbers[26] are always required. Up to date, plenty of metamaterial structures have been reported to demonstrate broadband perfect absorbers [27]. For instance, using hole array [28], cylinder array [29], complementary crosses and cylinders [30] and multilayer structures .

In this paper, we design an broadband absorber based on a multi-layer metamaterial nanostructure composed of a periodic array of silver-silica-silver (Ag-SiO2-Ag) cubes and a silver(Ag) bottom film. The proposed structure can achieve a nearly perfect absorption spanning a broad range from 600 nm to 1300 nm, indicating a wavelength band over 412 nm (>90%) from visible to near-infrared. In this band, the absorber exhibits an average absorbance of 97% and the peak absorbance of 99.8%. The broadband perfect absorption benefits from the excitation of surface plasmon resonance in addition

with the resonance induced by the metal-insulator-metal Fabry–Pérot (FP) cavity. The impact of the thicknesses of the top metal layer and the silica layer on the absorption performance is investigated in detail. Additionally, we thoroughly analyze the absorption properties of the metamaterials using various top and bottom metals, and the results demonstrate the effectiveness of the proposed structure. This structure is a polarization insensitivity absorber. The proposed metamaterial absorber not only has a simple geometry and ordinary metal based material composition, but also shows a high performance in both bandwidth and absorptivity. Moreover, this nanostructure is straightly compatible with high throughput manufacture technology using soft nano-imprinting lithography, making the low-cost mass-production of the material highly feasible. It is expected that such absorber structure will hold great potential in solar cell and photodetector applications.

## 2. Model and method

### 2.1. Model

The model structure of the wideband absorber is shown in the figure, in which (a) is a 3D structure diagram, and (b) is a side view of the structure. The electromagnetic absorber is composed of alternately stacked metal Ag and dielectric$Sio_2$, The unit cell period is P = Px = Py = 500 nm, The upper part is composed of cross structures with arm length equals arm width , Where the side length l = L = W = 170 nm, Thickness of metal layer $t_1 = t_2$ = 40 nm, The dielectric thickness in the middle is $d_1$ = 40 nm. The middle part of the unit is $Sio_2$ medium, Its thickness is $d_2$ = 70 nm, The bottom layer is a continuous Ag metal film, Its thickness $t_3$ = 120 nm. The numerical simulation is carried out using FDTD Solutions software. In terms of parameter setting, the periodic boundary conditions are set in both the x and y directions, and the perfect matching layer (PML) boundary conditions are set in the z direction. The grid accuracy is set to $\Delta x=\Delta y=\Delta z$=2 nm, In addition, the plane electromagnetic wave with the electric field E parallel to the x direction is incident along the -z direction, and the wavelength of the electromagnetic wave is taken to be 500-1300 nm.

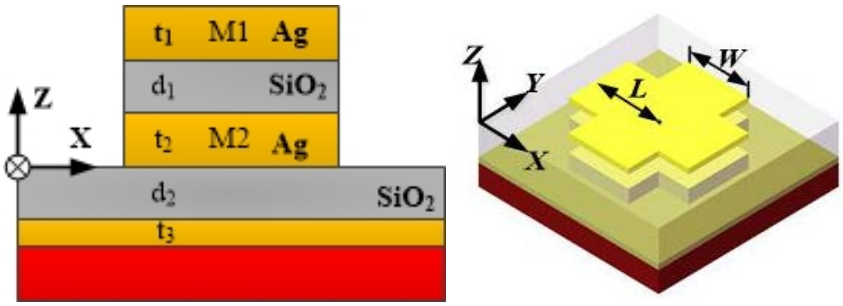


Fig 1. Metamaterial absorber model based on MDM structure

In the case of normal incidence of TM polarized electromagnetic waves, the broadband absorption spectrum shown in Fig 2. is obtained. The resonance wavelength corresponding to the P1 absorption peak in the figure is 554.9 nm, and the absorption rate reaches 97.5%. The absorption rates of the two obvious absorption peaks P2 and P3 in the broadband spectrum are 99.8% and 99.4%, respectively, and their corresponding wavelengths are 747.3 nm and 940.7 nm, respectively. It can be seen from the figure that for the above design parameters, the absorber exhibits good broadband absorption performance. From the absorption spectrum line, even in the concave part between the two absorption peaks, the corresponding minimum absorption rate is also 96% Above, the bandwidth of the absorption line absorption rate higher than 80% reaches about 300 nm, which greatly expands the application range of the absorber, which can be applied to solar cells, detectors , thermal emission Device and many other fields.

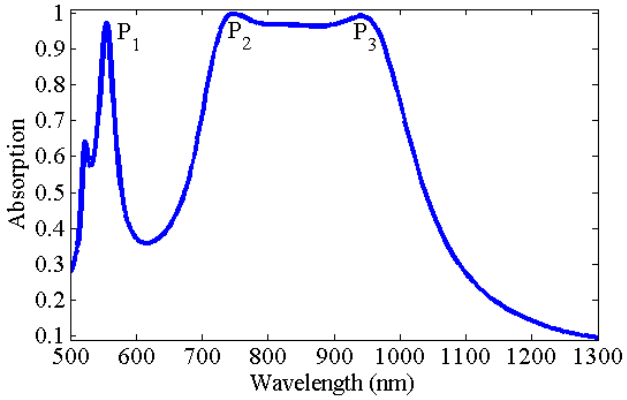


Fig 2. Broadband absorption peak

## 2.2. Method

Electromagnetic fields generated by the interaction between incident electromagnetic waves and such non-magnetic surface plasmon resonance metamaterials， can be described in detail by the Maxwell equations [13,14].

$$\nabla \times \vec{H} = \varepsilon_0 \varepsilon_r \partial \vec{E} / \partial t \tag{1}$$

$$\nabla \times \vec{E} = -\mu_0 \partial \vec{H} / \partial t \tag{2}$$

In the Maxwell equations， $\vec{H}$ and $\vec{E}$ represents the magnetic field strength and electric field strength respectively, $\varepsilon_r$ is representative of the dielectric permittivity of the dielectric material， $\varepsilon_0$ and $\mu_0$ represents the vacuum permittivity and vacuum permeability respectively. In the numerical simulation the optical properties of Ag nd $SiO_2$ were measured using the parameters of Olmon and Palik in the experiment.

Definition A is the absorptance of this absorber, this absorber for the surface plasmon resonance absorption loss of the incident electromagnetic wave can be defined by the equation.

$$A = 1 - T - R \tag{3}$$

## 3. Numerical analysis and discussion

Next, the absorption mechanism of the electromagnetic absorber is discussed. First, for the narrow-band absorption peak P1, since the side length of the upper square l = 170 nm, which is about 1/3 of the unit period, the spacing between the MDM array structures is very large, and the mutual influence is relatively weak, so this Absorption is caused by the interaction between the MDM structure and the underlying metal film. For the convenience of description, the upper metal of the MDM structure is defined as M1, and the lower metal is M2, as shown in Fig 1(c). When the incident wavelength is 554.9 nm, the distribution of the electric and magnetic fields corresponding to the absorption peak P1 is shown in Fig 3. It can be seen from the figure that there are strong enhanced electric fields on the left and right sides of the lower surface of the metal M2, and there is also a strong electric field distribution in the dielectric layer below the enhanced electric field, and the magnetic field is mainly distributed in the dielectric layer under the metal M2 . Therefore, when electromagnetic waves are incident, a large amount of charge is accumulated on both sides of the bottom edge of M2 and surface plasmon resonance (SPR) is generated. Since the dielectric layer is only 70 nm, the metal M2 also has a coupling effect with the underlying metal to jointly complete the incident electromagnetic Absorption.

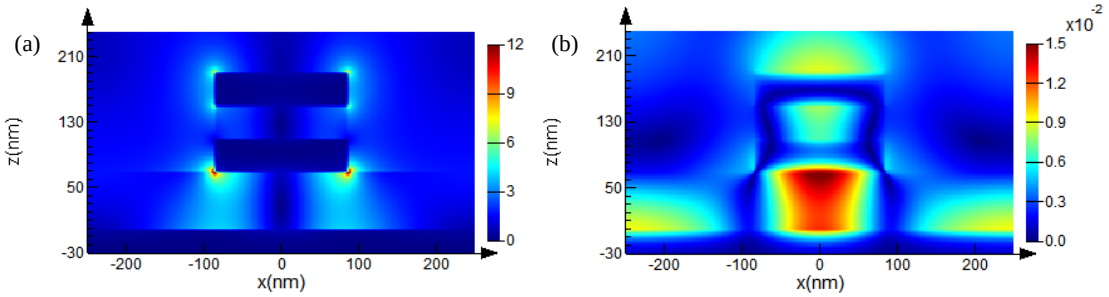


Fig 3. (A) Electric field and (b) magnetic field distribution at an incident wavelength of 554.9 nm

When the incident wavelength is 747.3 nm, the electromagnetic field distribution of the absorption peak P2 in the y = 0 plane is shown in Fig 4 (a) and (b). It can be seen from Fig4 (a) that the electric field is mainly distributed on both sides of the bottom edge of the metal M1 and the upper surface of the metal M2 at this time, and there are strong near the left and right regions of the dielectric layer between the metal M1 and M2 The electric field is distributed, while the magnetic field is mainly distributed within the dielectric layer of the MDM structure. From the point of view of the distribution characteristics of the electromagnetic field, the absorption of electromagnetic waves at this time is mainly affected by the MDM structure, and has little relationship with the dielectric layer and the underlying metal film under the MDM structure. When electromagnetic waves are incident, the oppositely polarized charges on the lower surface of the metal M1 and the upper surface of the M2 move to the left and right sides, gather near the edges of the two metal surfaces, and produce the local surface plasmon resonance (LSPR) phenomenon, thus A local enhancement of the electric field is caused near the sides of the metal surface. Due to the coupling effect of the enhanced electric field on the upper and lower metal surfaces, the electric field in the left and right regions of the dielectric layer is significantly enhanced. In addition, there is a certain intensity of electric field distribution on both sides of the lower surface of the metal M2, but it has little effect on the overall electromagnetic wave absorption. In addition, as can be seen from Fig 4(b), the magnetic field is mainly confined in the dielectric layer between M1 and M2. Therefore, for the absorption peak P2, the MDM structure plays a very important role in the electromagnetic absorption of metamaterials, forming a perfect absorption of nearly 100% of electromagnetic waves.

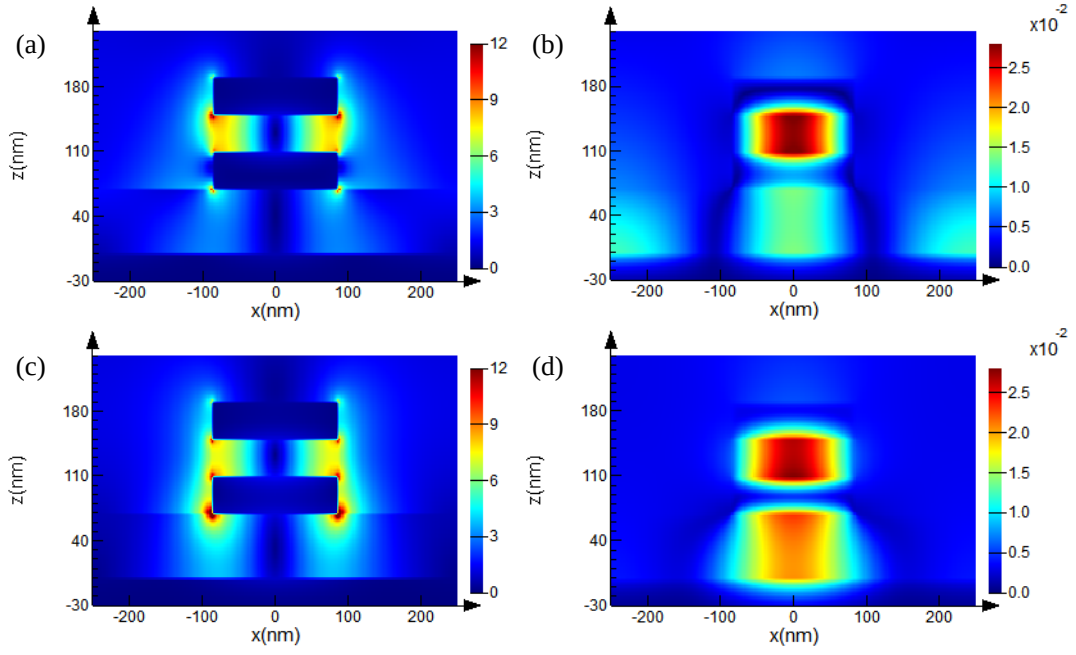


Fig 4. When the incident wavelength is 747.3 nm, the (a) electric field and (b) magnetic field distribution at the absorption peak P2, and when the incident wavelength is 940.7 nm, the (c)

electric field and (d) magnetic field distribution at the absorption peak P3, all of which are located at y = 0 in plane

### 3.1. Parameters

The structural size of the metamaterial is very important for the absorption of electromagnetic waves. With the modulation of the structural parameters, the equivalent impedance of the metamaterial may no longer match the impedance of the free space. Therefore, in the design process, the selection of the structural size is also Very critical. The effect of metal side length l on the broadband absorption of electromagnetic waves in the upper MDM structure is discussed below. As shown in Fig 5, while other parameters remain unchanged, when l = 140 nm, the absorption line is approximately single-band absorption. With the increase of the side length l, the bandwidth of the broadband absorption line gradually increases. But at the same time it is accompanied by a decrease in the absorption rate. Considering factors such as bandwidth and absorption rate, the side length l = 170 nm is an ideal choice. From the change trend of absorption spectrum, it can be discussed according to the LC equivalent circuit model theory . The change in side length l mainly affects the capacitances Cx and Cy, where Cx is the capacitance between two adjacent structural units, and Cy is the capacitance between two adjacent metal layers.

$$C_x \propto \frac{l}{P-ml},\ C_y \propto l^2$$

Where P is the unit period and m is a parameter related to the current distribution on the MDM end face parallel to the y-axis. And at this time, the resonance wavelength is proportional to the square root of the capacitance, so there are:

$$\lambda_1 \propto \sqrt{\frac{l}{P-ml}},\quad \lambda_2 \propto l$$

Therefore, with the increase of the side length l, the resonance wavelengths λ1, λ2 also increase, but the resonance wavelength increases at different speeds, so that the absorption spectrum is broadened, and the concave parts between the absorption peaks are also deepened .

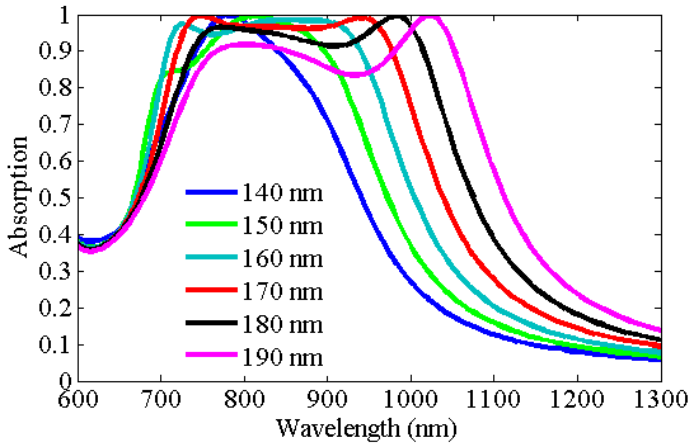


Fiig 5. Absorption rate varies with side length l

In addition to the metal side length l in the upper MDM structure affecting the absorption, the thickness of the dielectric layer in the structure can also affect the absorption of electromagnetic waves. When the dielectric thickness d1 in the MDM structure is changed alone, the change law of the absorption spectrum is shown in Fig 6 t can be seen that in addition to the green absorption curve, as the thickness d1 increases, the absorption peak P2 gradually decreases, and the corresponding resonance wavelength also tends to decrease. This is because the increase in the thickness d1 causes the capacitance between the upper and lower metal of the MDM structure to decrease, but the capacitance between the cells remains basically unchanged. Therefore, from the figure, the resonance wavelength corresponding to the absorption peak P3 is almost unchanged. Combined with the absorption peak P2 electromagnetic field and energy flow distribution, it can be seen that changing

the structure of MDM has a greater impact on the absorption of P2. When the thickness d2 of the dielectric layer changes, the structural absorption rate changes as shown in Fig 7. With the increase of d2, the capacitance between the metal M2 and the underlying metal film decreases, and the resonance wavelength corresponding to the absorption peak P3 gradually decreases, and the broadband absorption spectrum as a whole shows a decrease in the line bandwidth. It can be seen from the figure that when the thickness d2 of the dielectric layer is about 70 nm, the structure can obtain relatively ideal absorption, while also taking into account the requirements of the spectral line bandwidth.

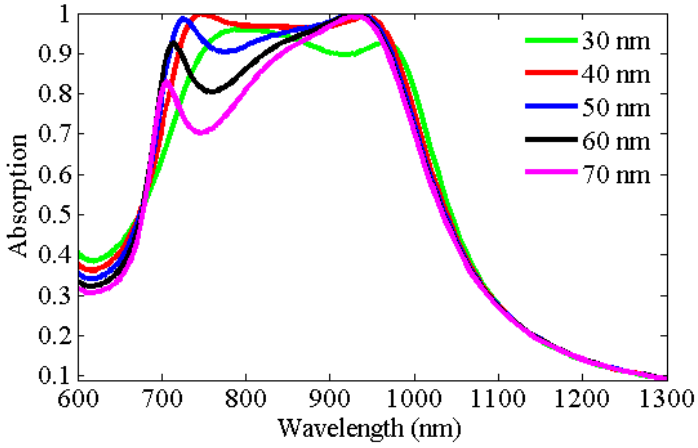


Fig 6. Absorption rate changes with d1

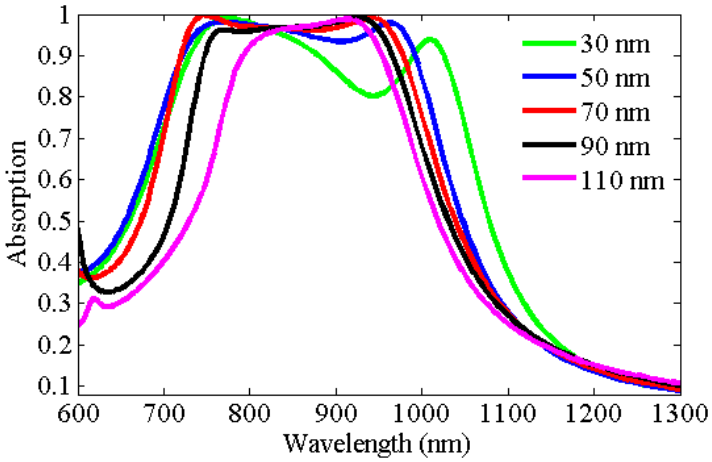


Fig 7. Absorption rate changes with d2

### 3.2. dieletric material

The choice of dielectric material will also have a great influence on the structural absorption. Fig 8 describes the change of the structural absorption rate with the dielectric refractive index n. It can be seen from the figure that with the increase of n, the broadband absorption line of the structure generally shows a red shift, and the bandwidth also continuously widens. When the refractive index n = 1.4, the center wavelength position of the absorption line is about 700 nm, but when n = 2.2, the center wavelength position of the absorption line is around 1 μm, and the spectral bandwidth increases, accompanied by structural absorption The rate of reduction. Due to the capacitance and the resonance wavelength, there is, that is, the resonance wavelength is proportional to the refractive index of the dielectric, so as n increases, the absorption line shifts to a longer wavelength, showing a red-shift trend. As can be seen from Fig8., the refractive index of $SiO_2$ in this structure is 1.76, which is relatively close to the red absorption line (n = 1.8). Considering the requirements of absorption rate and bandwidth, the selection of the dielectric material is in line with the ideal Happening.

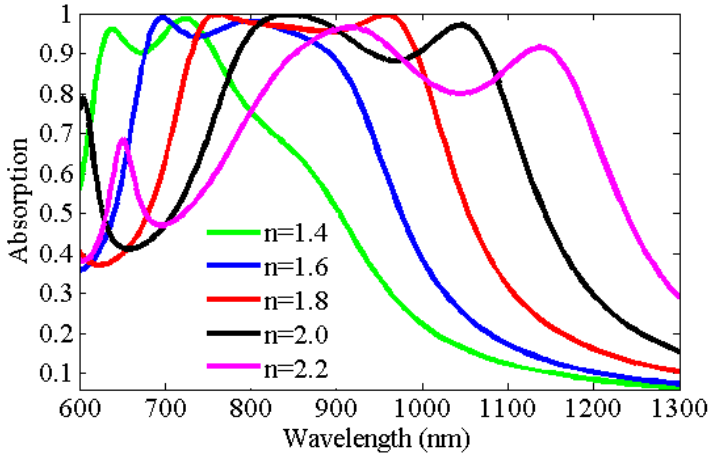


Fig 8. Absorptivity changes with medium refractive index n

## 4. Conclusion

In summary, In order to reduce the difficulty of processing the metamaterial structure, the paper have been proposed a designed a new two-dimensional metamaterial electromagnetic absorber based on the metal-dielectric-metal (MDM) structure. The device realized in the visible and near infrared bands of about 600~1300 nm Broadband absorption, the spectral line bandwidth with absorption rate higher than 80% reaches 412 nm. Further, the electromagnetic absorption mechanism of this metamaterial was analyzed. Combining the electromagnetic field distribution and energy flow density distribution, the physical mechanism of the structure's approximately perfect absorption of electromagnetic waves in a certain band was explained. Subsequently, the influence of structural parameters such as the length of the upper metal side, the thickness of the dielectric layer and the refractive index were discussed in detail. Based on this electromagnetic absorber, it has the advantages of simple structure and flat absorption spectrum, and it can play an important role in the fields of solar cells, detectors, thermal emitters and the like.

## References

[1] Zhigang L . Liliana S . Czaplewski D A , et al. “Wavelength-selective mid-infrared metamaterial absorbers with multiple tungsten cross resonators”. Optics Express, , 26(5):5616-5631(2018).

[2] Ayop O, Rahim M K A , Murad N A , et al. “Dual-band metamaterial perfect absorber with nearly polarization-independent”. Applied Physics A, , 123(1):63-70(2017).

[3] Shun Cao, TaiSheng Wang, Qiang Sun , et al. “Graphene-silver hybrid metamaterial for tunable and high absorption at mid-infrared waveband”. IEEE Photonics Technology Letters, PP(99):475-478(2018).

[4] Mohammadamir G , Karimi S E , Wolffenbuttel R F . “CMOS-compatible mid-IR metamaterial absorbers for out-of-band suppression in optical MEMS”. Optical Materials Express, 8(7):1696-1707(2018).

[5] Guo L , Ma X , Zou Y , et al. “Wide-angle infrared metamaterial absorber with near-unity absorbance. Optics & Laser Technology”, 98:247-251(2018).

[6] Lei L , Shun L , Haixuan H , et al. “Ultra-broadband absorber from visible to near-infrared using plasmonic metamaterial”. Optics Express, 26(5):5686-5693(2018).

[7] Chang L , Limei Q , Mingjing W . “Triple-broadband infrared metamaterial absorber with polarization-independent and wide-angle absorption”. Optical Materials Express, 8(8):2439-2448(2018).

[8] Xin L , Xiang Z , Lingling W , et al. “Enhanced dual-band absorption of molybdenum disulfide using a plasmonic perfect absorber”. Optics Express, , 26(9):11658-11666(2018).

[9] Zhang C , Huang C , Pu M , et al. Dual-band wide-angle metamaterial perfect absorber based on the combination of localized surface plasmon resonance and Helmholtz resonance. Scientific Reports, 7(1):5652-5657(2017).

[10] Kim J , Han K , Hahn J W . “Selective dual-band metamaterial perfect absorber for infrared stealth technology”. Scientific Reports, 7(1):6740-6748(2017).

[11] Yang J , Xu C , Qu S , et al. “Optical transparent infrared high absorption metamaterial absorbers”. Journal of Advanced Dielectrics, 08(1):1850007(1)-1850007(8)(2018).

[12] Zhang Y , Li T , Chen Q , et al. “Independently tunable dual-band perfect absorber based on graphene at mid-infrared frequencies”. Scientific Reports, 5:18463-18470(2015).

[13] Luo C , Ling F , Yao G , et al. “Dual-band tunable perfect metamaterial absorber in the THz range”. Optics Express, 24(2):1518-1527(2016).

[14] Zhao L , Liu H , He Z , et al. “Design of multi-narrowband metamaterial perfect absorbers in near-infrared band based on resonators asymmetric method and modified resonators stacked method”. Optics Communications, 420:95-103(2018).

[15] Lei Z , Han L , Zhihong H , et al. “Theoretical design of twelve-band infrared metamaterial perfect absorber by combining the dipole, quadrupole, and octopole plasmon resonance modes of four different ring-strip resonators”. Optics Express, 26(10):12838-12851(2018).

[16] S.-J. Li, P.-X. Wu, H.-X. Xu, Y.-L. Zhou, X.-Y. Cao, J.-F. Han, C. Zhang, H.- H. Yang, Z. Zhang, Ultra-wideband and polarization-insensitive perfect absorber using multilayer metamaterials, lumped resistors, and strong coupling effects, Nanoscale Res. Lett. 13, 386(2018).

[17] Bai Zhongyang, Liu Yongshan, et, al. Near-field Terahertz Sensing of Hela cells and Pseudomonas Based on Monolithic Integrated Metamaterials with Spintronic Terahertz Emitter. ACS Applied Materials & Interfaces., 10(20): 8543(2020).

[18] X. Hu, G. Xu, L. Wen, H. Wang, Y. Zhao, Y. Zhang, D. R. S. Cumming, and Q.Chen,“Metamaterial absorber integrated microfluidic terahertz sensors,” Laser Photonics Rev. 10(6), 962–969 (2016).

[19] Qingfang Zhong, Tao Wang, Xiaoyun Jiang, Le Cheng, Ruoqin Yan, Xing Huang. Near-infrared multi-narrowband absorber based on plasmonic nanopillar metamaterial. Opt. Commun. 19, 30861-2 (2019).

[20] Z. Zhou, T. Zhou, S. Zhang, Z. Shi, Y. Chen, W. Wan, X. Li, X. Chen, S. N. Gilbert Corder, Z. Fu, L. Chen, Y.Mao, J. Cao, F. G. Omenetto, M. Liu, H. Li, and T. H. Tao, “Multicolor T-ray imaging using multispectralmetamaterials,” Adv. Sci. (Weinh.) 5(7), 1700982 (2018).

[21] Yang Wang, Xue-Fei Xuan, Lu Zhu, Hai-Jun Yu, Qiang Gao, Xian-Lei Ge. Numerical study of an ultra-broadband, wide-angle, polarization-insensitive absorber in visible and infrared region. Optical Materials. 114, 110902 (2021).

[22] J. Schalch, G. Duan, X. Zhao, X. Zhang, and R. D. Averitt, “Terahertz metamaterial perfect absorber withcontinuously tunable air spacer layer,” Appl. Phys. Lett. 113(6), 61113 (2018).

[23] G. Duan, J. Schalch, X. Zhao, J. Zhang, R. D. Averitt, and X. Zhang, “Analysis of the thickness dependence of metamaterial absorbers at terahertz frequencies,” Opt. Express 26(3), 2242–2251 (2018).

[24] M. Born, and E. Wolf, Principle of Opics (Cambridge University, 1999).

[25] Yong Li, Xiang Zhai1, Sheng xuan Xia, Hong jian Li and Ling ling Wan. Active control of narrowband total absorption based on terahertz hybrid Dirac semimetal-graphene metamaterials. Journal of Physics D: Applied Physics. 122902, (2020).

[26] Zhao Xiaoguang, Duan Guangwu, Wu Ke, Anderson Stephan W., Zhang Xin. Intelligent Metamaterials Based on Nonlinearity for Magnetic Resonance Imaging. Advanced Materials., 5(4): 61-68(2019).

[27] W.-C. Chen, A. Cardin, M. Koirala, X. Liu, T. Tyler, K. G. West, C. M. Bingham, T. Starr, A. F. Starr, N. M. Jokerst, and W. J. Padilla, "Role of surface electromagnetic waves in metamaterial absorbers," Opt. Express 24(6), 6783–6792 (2016).

[28] Y. Hui, J. S. Gomez-Diaz, Z. Qian, A. Alù, and M. Rinaldi, "Plasmonic piezoelectric nanomechanical resonator for spectrally selective infrared sensing," Nat. Commun. 7(1), 11249 (2016).

[29] J. A. Mason, S. Smith, and D. Wasserman, "Strong absorption and selective thermal emission from a midinfrared metamaterial," Appl. Phys. Lett. 98(24), 241105 (2011).

[30] L. Li, "New formulation of the Fourier modal method for crossed surface-relief gratings," J. Opt. Soc. Am. A 14(10), 2758–2767 (1997).